Postprint of: Hoja J., Lentka G., Interface circuit for impedance sensors using two specialized single-chip microsystems, Sensors and Actuators A: Physical, Vol. 163, Iss. 1 (2010), pp. 191-197, DOI: 10.1016/j.sna.2010.08.002

Jerzy Hoja was born in Poland in 1947.
He received the M.Sc. and Ph.D. degrees in electronic instrumentation from the Faculty of Electronics, Telecommunications and Informatics, Gdansk University of Technology, Gdansk, Poland, in 1970 and 1979, respectively. He is currently Lecturer and Researcher with Department of Optoelectronics and Electronic Systems, Gdansk University of Technology. His research interests include impedance measurement, design of measurement and diagnostic systems for electronic circuits and objects modeled by electrical circuits.

Grzegorz Lentka was born in Poland in 1972.
He received the M.Sc. and Ph.D. degrees in measurement systems from the Faculty of Electronics, Telecommunications and Informatics, Gdansk University of Technology, Gdansk, Poland, in 1996 and 2003, respectively. He is currently an Assistant Professor and Researcher with Department of Optoelectronics and Electronic Systems, Gdansk University of Technology. His research interests include digital signal processing, impedance measurement, design of measurement and diagnostic systems for electronic circuits and objects modeled by electrical circuits, systems on a chip.

Interface circuit for impedance sensors using two specialized single-chip microsystems

Jerzy Hoja [a)], **Grzegorz Lentka** [b)]

[a)]Gdansk University of Technology, Faculty of Electronics, Telecommunications and Informatics, Poland, 80-233 Gdansk, Narutowicza 11/12, hoja@eti.pg.gda.pl
[b)]Gdansk University of Technology, Faculty of Electronics, Telecommunications and Informatics, Poland, 80-233 Gdansk, Narutowicza 11/12, lentka@eti.pg.gda.pl, tel. +48-58-347-2197, fax. +48-58-347-2255

Abstract

The paper presents an interface circuit designed for the measurement of impedance parameters of sensors or measurement cells installed on technical objects. The interface circuit allows measurement of the modulus and argument of impedance in the range of 10 Ω ≤ $|Z_x|$ ≤ 10 GΩ at a measurement frequency in the range of 0.01Hz ÷ 100 kHz. The new solution based on two specialized SoC AD5933 microsystems has been used. This has allowed to obtain miniaturization, low power consumption and low-cost of the circuit of the impedance interface. During tests of the realized prototype using the reference object, the object impedance measurement errors have been determined and they do not exceed ±1.6% (for relative error of impedance modulus) and ±0.6° (for absolute error of impedance argument). The obtained accuracy is fully acceptable in case of impedance measurement of anticorrosion coating in the field. The comparison measurements performed with the aid of Solartron set of instruments showed that the impedance measurement accuracy of the proposed module is comparable to laboratory set of instruments.The important advantage of the used solution based on AD5933 microsystems is lowering the power consumption down to ca. 0.7 W, which makes possible powering the measurement module from a PC using +5V from the USB. It is a very profitable feature for a module designed to work directly in the field.

1. Introduction

There are many technical and biological objects, the parameters of which are determined by impedance measurement. An example of such approach is monitoring and diagnostics of anticorrosion protection (anticorrosion coatings) of large technical objects like pipelines, bridges, fuel tanks etc. on the basis of impedance measurement of the protective coatings [1-3]. When using medical sensors, the impedance measurement can be applied for testing of tissues, physiological liquids, skin etc. in order to diagnose the state of disease of organs [4-6]. An example of environmental protection and safety is the use of impedance measurement for monitoring of water percolation of dikes [7-9].

The above mentioned examples show that there is quite a number of applications of impedance measurement for testing of different objects in real-life conditions. The measurements are performed using impedance sensors or measurement cells connected to a measurement circuit located near the tested object (often directly in the field, in difficult-to-reach places). This requires to design the measurement circuit in the form of an interface circuit which estimates impedance parameters and sends them to the controlling computer. This implies the need of miniaturization, low power consumption and ability to work in difficult environment conditions. The interface with such features is the subject of the paper. The

use of specialized energy-efficient electronic chips of highest-scale integration e.g. SoC microsystems (AD5933), microcontrollers (AT32UC3B1256), and also the use of measurement methods based on digital signal processing (DSP) [10] were necessary to realize the interface.

2. Sensors

One of the most important fields of the use of impedance measurement in the industry (economy) is the monitoring of anticorrosion protection of the different objects due to huge losses caused by corrosion. Also due to safety reasons, it is necessary to determine the condition of the anticorrosion coatings in order to estimate the time of renovation. This extorts the need of the impedance measurement of the coating and diagnose their performance, also in the field, directly on the protected object using a sensor – measurement cell.

2.1. Equivalent circuit model

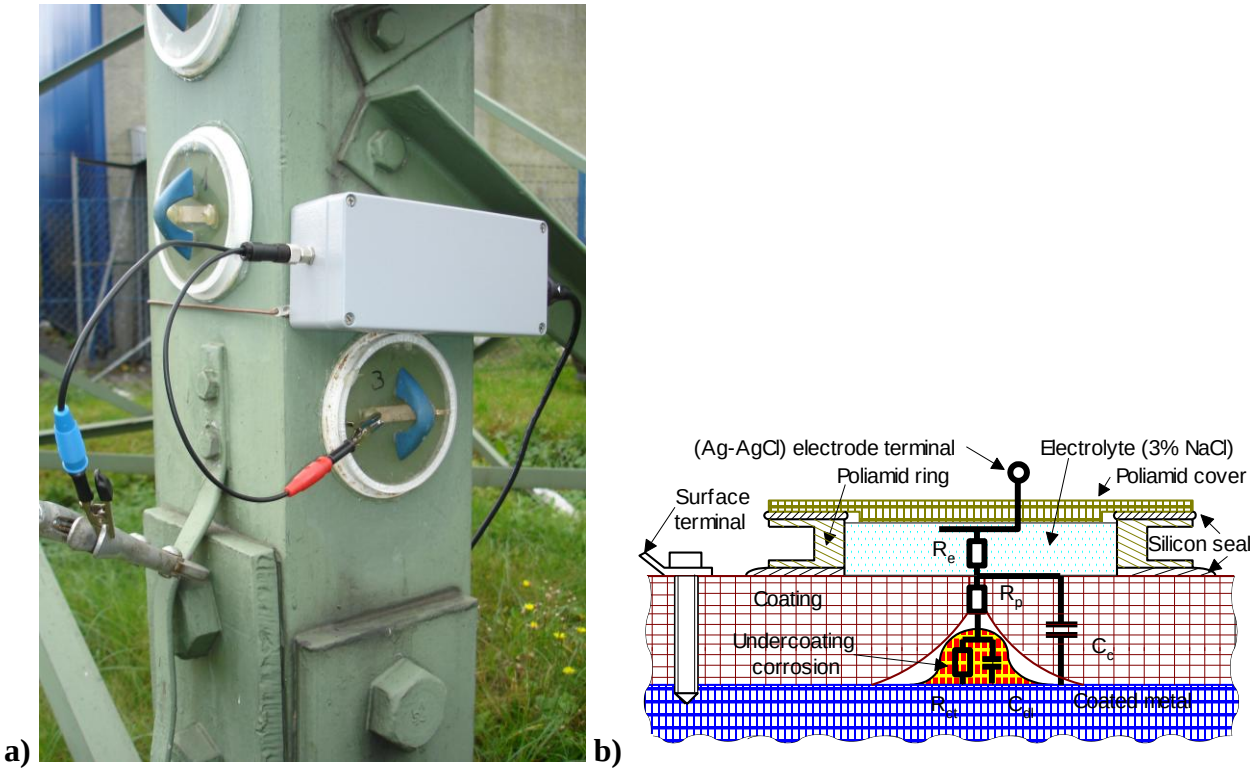

Fig. 1. a) The photography of cells for impedance measurement of anticorrosion coatings on a high-voltage pylon b) Cross-section of the anticorrosion coating and the measurement cell

The view of the cell located on a high-voltage pylon and connected to the impedance interface is shown in Fig.1a, and a cross-section of the coating and the cell in Fig. 1b [11]. When the coating is new and the protection is based on the barrier mechanism, there is no penetration of electrolyte into the coating and the equivalent circuit contains only two elements: capacitance C_c (of the order of a few tens – a few hundreds pF) and resistance R_p (a few, up to several hundreds GΩ) modelling properties of the material of the coating (the electrolyte resistance R_e is much smaller and practically negligible). After some time, the coating loses the barrier protection and the electrolyte starts to penetrate the coating, but the coating still has adhesion properties and there is no undercoating corrosion. At this stage, the electrolyte in the pores influences the R_p, the value of which is decreasing more and more when the electrolyte penetrates the coating. Additionally, the electrolyte penetration of the coating causes the increase of the dielectric constant, which leads to an increase of the capacitance C_c. At the next stage, the coating is broken and the undercoating corrosion appears. The equivalent circuit is extended by new

elements: double layer capacitance C_{dl} and charge transfer resistance R_{ct}. Following the corrosion's expansion, the value of R_p is continuously decreasing and finally the coating is destroyed and the equivalent circuit contains only R_{ct} and C_{dl}.

Resuming, the knowledge of the above-mentioned parameters allows to estimate the quality of the anticorrosion coating and to avoid corrosion-caused losses. The difficulty of coating equivalent circuit identification lies in the fact that the RC elements are differing considerably in their values and elements with small and large values are shunting each other. Thus, for the identification of the components, the impedance measurement is required in a wide frequency range, starting from very low, of the order of mHz up to MHz, which is called impedance spectroscopy.

2.2. Impedance spectroscopy

An example of the modulus ($|Z|$) and argument ($\arg(Z)$) characteristic of the impedance of a high-thickness anticorrosion coating in the early stage of the undercoating rusting, is presented in Fig. 2. It is a very important moment, because the immediate renovation of the coating can stop the corrosion.

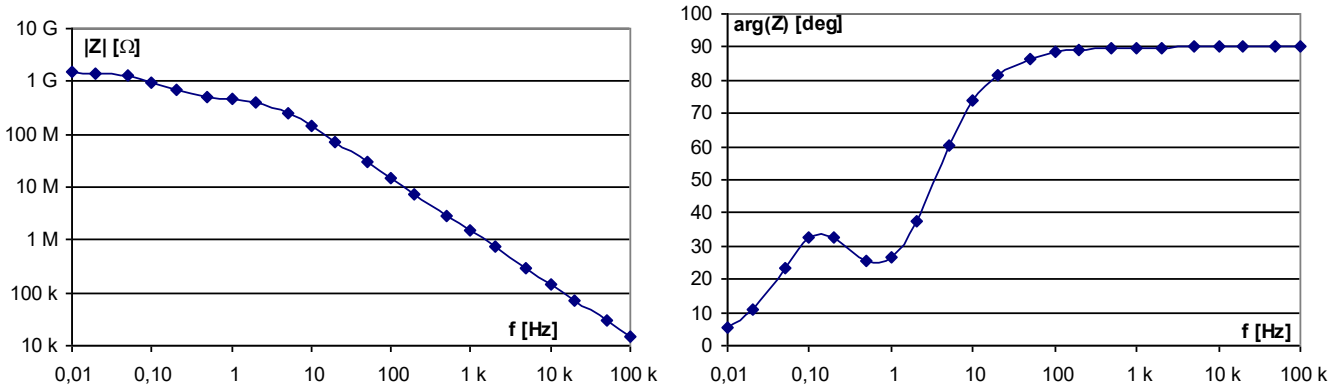

Fig. 2. Exemplary modulus and argument graphs of the impedance of the anticorrosion coating

The characteristic inflection of curves in the frequency range of 10 Hz – 0.1 Hz points out that the equivalent circuit contains elements C_{dl} and R_{ct}, showing the undercoating corrosion is at the early stage. For the identification of the parameters of the equivalent circuit of the coating, the most effective is the method using an impedance spectroscopy.

In the impedance spectroscopy technique, two steps can be distinguished: the measurement and an analysis. In the first one, the vector measurement of impedance Z is performed in a wide frequency range to determine real $\mathrm{Re}(Z)$ and imaginary $\mathrm{Im}(Z)$ parts or modulus $|Z|$ and argument $\arg(Z)$ of impedance, using contact electrodes or a measurement cell placed on the tested object. In the second step – an analytical one, on the basis of the impedance spectrum, the parametric identification of the model (in most cases in the form of a multi-element RC two-terminal network) is made using CNLS (Complex Nonlinear Least Square) method for fitting the model to the experimental spectrum [12-14].

In this paper we deal with the main difficulties and problems lying in the measurement stage. They arise from the necessity of the measurements in a wide frequency range and also from the need to adapt to test objects in real-life conditions directly in the field. This implies the need of miniaturization, low power consumption and ability to work in difficult environment conditions while assuring metrological parameters comparable to laboratory impedance analyzers [15-17]. On the market, there are no commercially available impedance analyzers miniaturized enough and allowing telemetric communication between measurement module installed near the sensor on the object and a personal computer used to control measurement module. The paper presents a developed miniaturized impedance measurement module, which uses a single-chip AD5933 microsystem (SoC) from Analog Devices chosen on the basis of the analysis of the newest VLSI chip market.

3. Interface circuit

The undoubtful advantages of the AD5933 chip are low power consumption and integration of most blocks required for impedance spectroscopy. It contains a sinusoidal signal generator, an A/D converter and a hardware DFT calculation module. The performed analysis and tests of the circuit in the configuration suggested by the manufacturer [18] show its limitations when using it as an impedance analyzer. As the most important, the following disadvantages can be counted: narrow measurement range of modulus (1 kΩ ÷ 10 MΩ) and narrow range of measurement frequency (1 kHz ÷ 100 kHz), the need of performing a calibration measurement, variable output resistance. Because of these facts, the solution of the circuit of impedance interface based on the new, original configuration using two AD5933 chips and an extended input circuitry was proposed.

3.1. Architecture

The AD5933 chip contains analog blocks as well as digital ones necessary for measuring impedance by the method based on the DSP technique (block diagram of the AD5933 is part of the schematic shown in Fig. 3). The SoC is equipped with an I^2C interface used to control the chip and to read internal registers of the microsystem. Unfortunately, the I^2C address of the SoC is fixed by the manufacturer and does not allow to connect more than one chip to the same I^2C bus. In the SoC, two channels can be observed: one for the generation of the excitation signal and the second for determination of the orthogonal parts of the measurement signal. The sinusoidal signal generation is based on the direct digital synthesis (DDS) method. The channel consists of the 27-bit DDS core, a D/A converter and a programmable-gain amplifier A1 with output resistance R_{out}. In the measurement channel, the signal from amplifier A2 is applied to a low-pass filter (antialiasing), and then sampled and quantized by a 12-bit A/D converter. The calculation of the real and imaginary parts of the signal is performed by the discrete Fourier transformation (DFT) module on the basis of collected samples.

The main disadvantage of the configuration proposed by the manufacturer is the use of only one AD5933 chip allowing to measure only orthogonal parts of current flowing through the measured impedance [19]. Because, in order to calculate the impedance it is necessary to know the voltage across the measured impedance, the manufacturer assumes two measurement cycles: calibration and normal. During the calibration measurement, the reference resistor R_{cal} is connected instead of the measured impedance, allowing to estimate the voltage across the measured impedance. The two-cycle algorithm proposed by the manufacturer is onerous to realize and also leads to very large errors [20]. In the developed measurement circuit, a simultaneous measurement of the voltage across and current through was proposed (thus eliminating the need of the calibration cycle), using two AD5933 chips in the new configuration different from that recommended in the manufacturer's application note. The block diagram of the developed impedance interface is presented in Fig. 3.

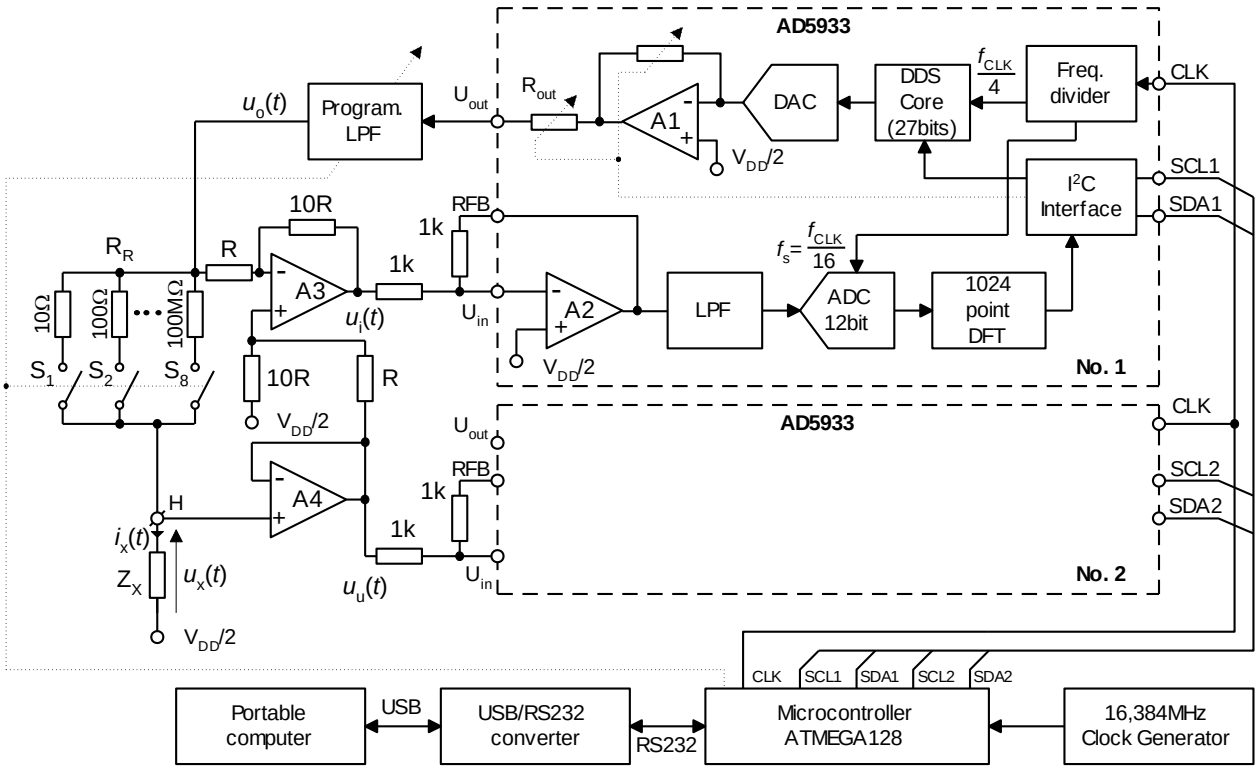

Fig. 3. Block diagram of the circuit for impedance measurement.

One of the SoCs was used for generation of the excitation signal and for determination of the orthogonal parts of the signal $u_i(t)$ proportional to the current flowing through Z_x. The second SoC realizes the measurement of the Re and Im parts of signal $u_u(t)$ proportional to the voltage across the measured impedance Z_x.

The extraction of the signals $u_u(t)$ and $u_i(t)$ is performed in the input circuitry (amplifiers A3 ÷ A4) connected to SoC chips. For the current measurement, a differential amplifier (A3) with gain equal to 10 was used, but the voltage is measured with the aid of a voltage follower (A4). Amplifiers A2 in both AD5933 chips work with a gain of –1 thanks to externally connected 1 kΩ resistors. In the realized interface the measured impedance is calculated using the definition on the basis of the formulas:

$$|Z_x| = 10 R_R \sqrt{\frac{(\mathrm{Re}U_u)^2 + (\mathrm{Im}U_u)^2}{(\mathrm{Re}U_i)^2 + (\mathrm{Im}U_i)^2}} \quad , \tag{1}$$

$$\varphi_{Z_x} = arctg\frac{\mathrm{Im}U_u}{\mathrm{Re}U_u} - arctg\frac{\mathrm{Im}U_i}{\mathrm{Re}U_i} \tag{2}$$

where: R_R – current measurement range resistance,

$\mathrm{Re}U_u$, $\mathrm{Im}U_u$ and $\mathrm{Re}U_i$, $\mathrm{Im}U_i$ orthogonal parts of signals $u_u(t)$ and $u_i(t)$ read from SoC registers.

The manufacturer of AD5933 assumes that the impedance measurement is realized by only one SoC, so all chips have the same I²C address and do not have pins/inputs to modify the address. So it is impossible to connect two (or more) AD5933 to the same I²C bus at the same time. Two separate I²C busses were arranged to control two SoCs, but some problems weren't solved. The sequential driving of the chips caused that each SoC has started measurement signal generation in the different moment of time. As a result, the impedance, calculated on the basis of formulas (1 - modulus) and (2 - phase) as a ratio of results (of voltage $u_u(t)$ and current $u_i(t)$) measured by each AD5933, has random phase, because the coordinate system for determining orthogonal parts of signal by DFT operation is related to its DDS generator. In order to eliminate this unwanted phenomena, it was necessary to use the same clock (CLK) for both chips and synchronous sending of commands to both chips, which makes possible starting

measurement sequence at the same time. It was obtained by software emulation of two I^2C busses realized on one I/O port of microcontroller.

3.2. Construction

The developed input circuitry of the interface allows impedance measurement of the anticorrosion coatings on grounded objects. In order to measure high impedances (up to $|Z_x| \leq 10$ GΩ), the amplifiers in the input circuitry must be characterized by low input currents (on the level of few pA) and high differential and common input impedance (Z_{dif}, Z_{cm}) while assuming the possibly widest bandwidth. Because the input amplifiers of the AD5933 do not meet these requirements the interface was extended by external input circuitry (A3 ÷ A4). The AD8646 amplifiers were used, whose input currents do not exceed 1 pA (at temp. 25°) and the impedances Z_{dif} and Z_{cm} are determined by resistances $R_{dif} = R_{cm} = 10$ TΩ and capacitances $C_{dif} = 2.5$ pF and $C_{cm} = 7.8$ pF and the wide bandwidth GBW = 24 MHz.

Range resistor R_R connected in series with Z_x serves for the measurement of the current i_x flowing through Z_x. To assure a wide measurement range of impedance Z_x (current i_x changes from 10 pA to 1 mA), the range resistors R_R (10 Ω ... 100 MΩ) switched in decades by miniature reed-relays were used. The value of the range resistor R_R is chosen in relation to $|Z_x|$ of the measured coating according to criterion: $0.01|Z_x| < R_R \leq 0.1|Z_x|$. Assuring this condition means that the resistance R_R is lower than $|Z_x|$ at least by an order and causes at least ten times lower impedance seen from terminal H in relation to ground. It is profitable for decreasing noise appearing on the impedance Z_x, but requires additional amplification ×10 of signal from R_R. This way, the amplitude of signal $u_i(t)$ is comparable to the amplitude of signal $u_u(t)$, taken directly from the unknown impedance Z_x with the aid of voltage follower A4.

Using an internal clock source, the AD5933 chip allows to measure the impedance spectrum in the frequency range of 1 kHz ÷ 100 kHz. For impedance spectroscopy the required measurement frequency range is much wider. The construction of the AD5933 allows to use an external clock source, which makes possible clock scaling and finally generation of the signal at frequencies below 1 kHz.

When designing the ranges of generated measurement frequencies, it is necessary to select such clock frequencies f_{clk}, which will allow to obtain a frequency grid f_m in the range of 0.1 Hz÷ 100 kHz (10 frequencies with a fixed step Δf_m in each decade), for which there is no spectrum leakage. Also the time of acquisition of 1024 samples (T_{meas}) of measurement signals u_u and u_i in order to perform DFT influences the selection of f_{clk}. If $T_{meas} = 20$ ms or when it will be a multiple of the period of noising signal appearing from the power network (50 Hz), the influence of the noising signal will be eliminated in the DFT process. This requirement is very important in case of the measurement of very high impedances ($|Z_x| > 10$ MΩ), at frequencies $f_m < 1$ kHz.

The AD5933 chip is dedicated for impedance spectroscopy. To do this, the manufacturer assumes the frequency sweeping realized by increasing current measurement signal frequency by the value given in the frequency increment register. This way, it is possible to use maximum of 511 steps of frequency increment. The AD5933 has also starting frequency register which determines first frequency in the sweep. In case of using two AD5933 chips, which require synchronous controlling, the authors have omitted this possibility. The measurement at each frequency, from the AD5933 point of view, is separated by new command. After each measurement, the Reset command is executed, which initializes chip like after power on. The SoCs work with external clock source, the frequency of which is set by microcontroller before resetting SoC. Performing Reset before each measurement at the selected frequency assures full synchronization of the measurement channels for current and voltage realized with the aid of two AD5933 chips.

Taking into account relations between f_{clk}, f_m and f_s (Fig. 3), an external clock source was assumed with a frequency of 16.384 MHz, which is divided by the microcontroller allowing to obtain six values of f_{clk} fulfilling the above conditions. Table 1 shows the parameters of the generated measurement signal and the number of periods (L) and time T_{meas} of acquisition of signal samples.

Table 1. Measurement signal parameters

f_{clk} [Hz]	f_m [Hz]	Δf_m [Hz]	L	T_{meas} [s]
8.192 M	10 k-100 k	10 k	20-200	2 m
819.2 k	1 k-9 k	1 k	20-180	20 m
	100-900	100	2-18	
81.92	10-90	10	2-18	0.2
8.192 k	1-9	1	2-18	2
819.2	0.1-0.9	0.1	2-18	20
81.92	0.01-0.09	0.01	2-18	200

According to the DDS rule, in each frequency decade the sinusoidal signal $u_o(t)$ is approximated using a different number of samples in a period. The number of approximating steps in the period of the generated signal varies from 2048 (for the lowest frequency in each decade) down to about 22 for the highest frequency. When using such type of signal to measure impedance Z_x in the circuit presented in Fig. 3, a differentiation of the slopes of each step can appear. In order to decrease the influence of the noising impulses, an additional low-pass filter with a band-pass frequency switched in decades was used at the output of the SoC, making the generated signal $u_o(t)$ much cleaner.

The view of the realized device with the measurement cells located on the construction of the high-voltage pylon is shown in Fig. 1a. Figure 4 presents the internal construction of the measurement module. The input circuitry can be seen as a separate PCB placed on the baseboard. The used solution allows replacement of the input circuitry depending on the impedance parameters of the tested object.

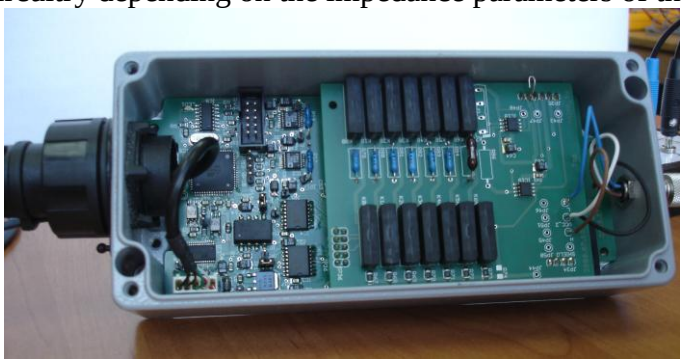

Fig. 4. View of the internal construction of the impedance measurement module.

The prototype of the module was realized in the form of a virtual instrument. A personal computer was used to control the measurement module via USB. A graphical user interface (GUI) was designed (Fig. 5).

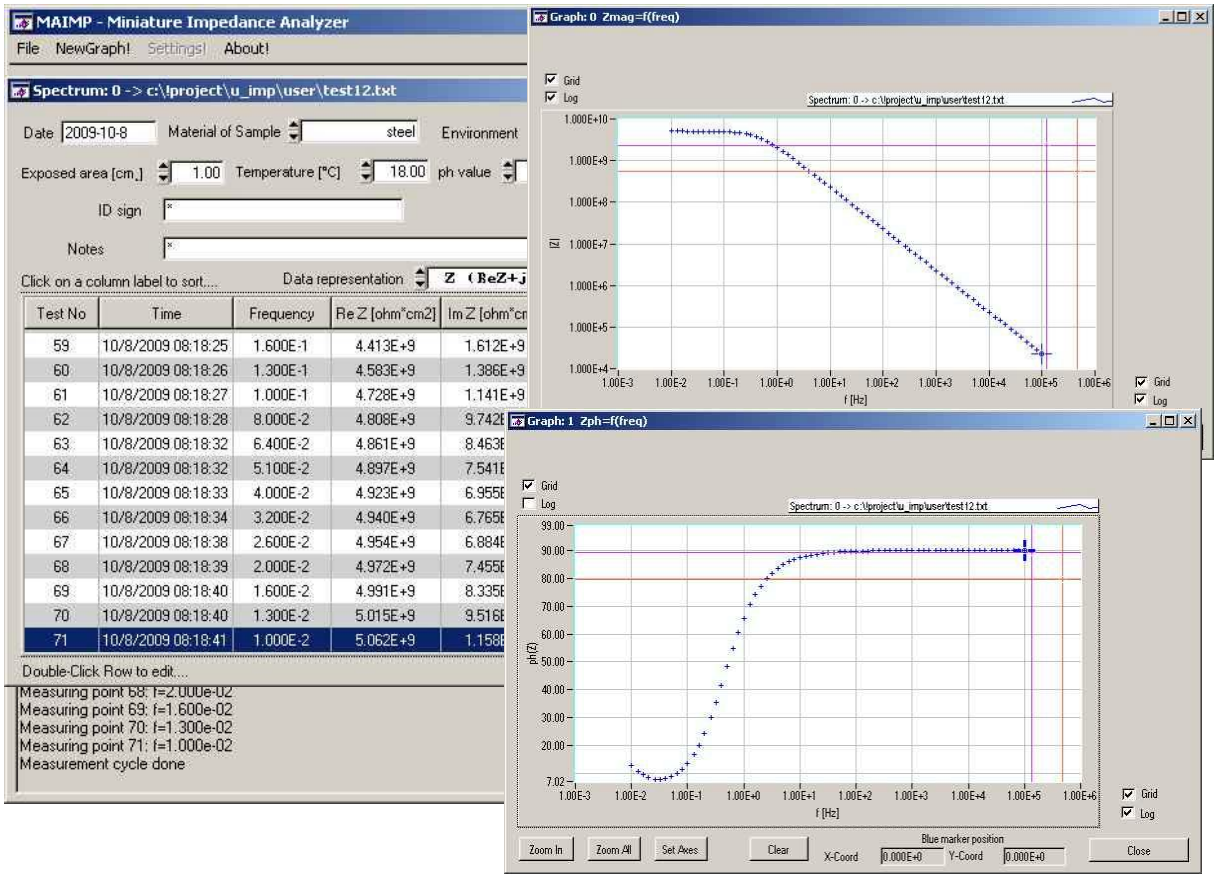

Fig. 5. Graphical user interface controlling the impedance measurement module

The GUI allows to program parameters of the measurement (amplitude and frequency of the measurement signal) and display of the measured value of the modulus and argument of the impedance of the tested object (calculated in the PC on the basis of (1-3). For the presentation of the results of impedance spectroscopy of the object in the form of a Bode plot of modulus and argument of impedance as a function of the frequency, separate windows were designed in the GUI.

4. Experimental results

Tests of the realized device were made using the reference two-terminal RC network shown in Fig. 6. The configuration and the values of the components are a typical example of the equivalent circuit of the impedance of anticorrosion coating in the early stage of exploitation (the impedance modulus reaches 1.5 GΩ at low frequencies).

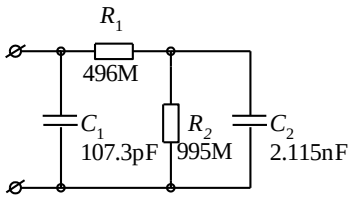

Fig. 6. Electrical diagram of the reference two-terminal RC network.

The selected two-terminal RC network is a good example of the use of impedance spectroscopy for diagnostics of anticorrosion coatings of objects located in the field. The capacitors were measured using an E4980A precise impedance meter with an error does not exceeding 0.1%, but resistors were measured with the aid of the technical method using a reference resistor of 10 MΩ ±0.01% and a 34401A multimeter.

Ten measurement series of the impedance of the two-terminal network were carried out for frequencies in range of 100 kHz – 0.01 Hz (with 1-2-5 steps), using a signal with $1V_{RMS}$ amplitude. The mean values for the obtained results of modulus and argument of impedance were calculated. For each measurement point the standard deviation for the impedance modulus does not exceed 0.1%, and for the argument it is lower than 0.1°.

The use of formulas (1) and (2) to determine the parameters of the measured impedance is correct when assuming that the signals $u_u(t)$ and $u_i(t)$ extracted in the input circuitry and then processed to a digital value in SoCs are dependent only on the current i_x through and the voltage u_x across Z_x. In real-life conditions, the signals u_i and u_u are also influenced by the unwanted phenomena (e. g. parasitic capacitances, real-life parameters of the operational amplifier used as a voltage-follower etc.) causing impedance measurement errors. The analysis of above mentioned errors of the input circuitry in the used configuration was done in [21]. It was shown, that the input circuitry mainly influences the accuracy of the impedance measurement, so, there is a need of using a correction formula to correct signals extracted in the input circuitry. Taking into account the above, the correction formula was developed Z_m:

$$Z_m = -\left\{ \frac{1}{10 \cdot Z_R} \cdot \frac{1+\frac{11}{A_u}}{\mathrm{Re}\left(\frac{U_u}{U_i}\right) + j\,\mathrm{Im}\left(\frac{U_u}{U_i}\right)} + Y \right\}^{-1} \tag{3}$$

where: $Z_R = \dfrac{1}{\dfrac{1}{R_R} + j\omega C_R}$ - the impedance formed by parallel connection of the range resistor R_R and capacitance C_R introduced by reed-relays performing range change and by layout capacitances,

$A_u = \dfrac{A_{DC}}{1 + j\dfrac{\omega}{\omega_{3dB}}}$ - is the single-pole (ω_{3dB}) transfer function of amplifier A3, A_{DC} – DC open-loop gain of the amplifier [22],

$Y = \dfrac{1}{R_{dif}} + \dfrac{1}{R_{cm}} + j\omega\left(C_p + C_{dif} + C_{cm}\right)$, C_p –capacitance introduced by cables connecting the impedance Z_x to voltage-follower A4,

The capacitance C_R is resulting from parasitic capacitance of reference resistor, capacitance of reed relays and layout capacitances. The highest resistor 100M type GS-1/2 manufactured by TAMA is made in thick film technology, and its parasitic capacitance is 0.24pF measured with Agilent LCR Meter E4980A. Capacitance across contacts of reed-relay (manufactured by MEDER with switch KSK-1A72 FORM A (single contact)) is 0.2pF (catalog data).

The parasitic capacitance is mostly important in case of the highest range resistor of 100MΩ. In this case, the resultant capacitance is the sum of self-capacitance of resistor 100MΩ (0.24pF) and 7 resultant capacitances for other 7 range resistors which can be connected with relay (the relays are open at this time). These capacitances are created from connecting in series capacitance of each resistor and capacitance of respective reed relay (7 * [0.24pF in series with 0.2pF] = 0.77pF). Finally, it gives summary capacitance C_R of about 1pF.

The used reed-relays are characterized by low resistance in the on-state $R_{on} \leq 100$ mΩ. In the worst case, when the switch S_1 connects range resistor with the smallest resistance $R_R = 10$ Ω, the resistance R_{on} causes an error of 0.1%. Because the range resistors have a tolerance of 0.1%, the maximal error of the range resistor can be assumed as 0.2%.

The relative error of modulus ($\delta_{|Z|}$) and absolute error of argument ($\varepsilon_{arg(Z)}$) of impedance of the tested two-terminal network were calculated assuming the impedance calculated theoretically on the basis of the values of reference components as a real one, the measured impedance was calculated using (3) (Fig. 7). Relative error of two-terminal network impedance modulus is in the range of ±1.6%, and the absolute error of argument ±0.6°, respectively (excluding the highest frequency point).

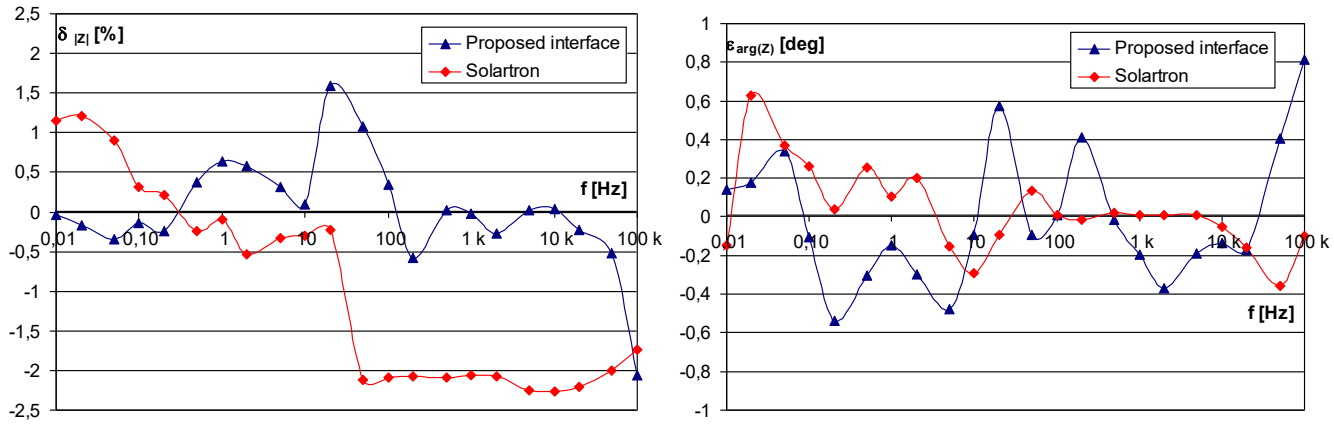

Fig.7. Relative error of modulus and absolute error of argument of the impedance of the reference two-terminal RC network.

When analysing the graphs, the increase of errors at frequencies above 10 kHz can be noticed. It is caused by the non-symmetrical channels for measurement of current and voltage on Z_x. In the whole frequency range, a cyclical increase and decrease of errors connected with the varying sampling frequency of generation of the measurement signal (using DDS method) can be observed. The influence of the changing number of samples in the period of the generated excitation signal is visible.

In order to fully evaluate the realized interface, the reference two-terminal RC network (Fig. 6) was also measured using set of Solartron instruments: 1255 FRA and 1294 Impedance Interface. The measurement was carried out in the same conditions like the developed circuit and the obtained results were shown in Fig. 7. The analysis of error curves allows to notice that the developed module is characterized by the accuracy on the same level like the Solartron set.

In order to evaluate the usefulness of the measurement module for diagnostics of anticorrosion coatings in the field, the impedance of the painted coating on a high-voltage pylon was measured. The tests were performed using two measurement cells with 80 cm^2 surface each, sequentially connected to the input terminals of the interface circuit. The cells represent two kinds of the tested painted anticorrosion coatings. The curve marked □ shows a coating with good quality, but the curve marked by Δ represents a coating with numerous pores, where the penetrating electrolyte caused a meaningful decrease of the coating resistance R_p. The view of the measurement set is shown in Fig. 8.

Fig. 8. Impedance measurements in the field of the anticorrosion coating on a high-voltage pylon, using the interface circuit powered and controlled by portable computer via USB

The comparison measurements were performed using an ATLAS 0441 impedance analyzer [23]. The results are presented in Fig. 9.

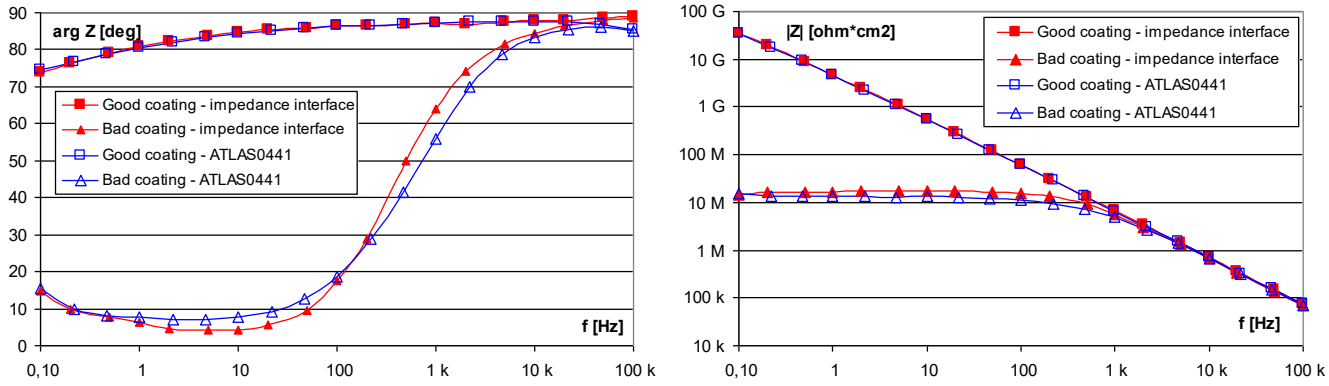

Fig. 9. The graph of modulus and argument of the impedance of the anticorrosion coating for two measurement cells, measured using the impedance interface and the ATLAS 0441 analyzer.

The graphs shows very good correlation of results obtained with the aid of both instruments. The obtained accuracy is better than required for the coating impedance measurement performed in the field.

5. Conclusion

A miniaturized measurement module for impedance spectroscopy of different objects modelled by multi-element two-terminal RC networks was developed. It measures impedance in the range of $100\ \Omega \le |Z_x| \le 10\ G\Omega$ at measurement frequencies in the range of $0.1Hz \div 100\ kHz$ (10 frequencies in

each decade). A new solution based on two specialized AD5933 microsystems SoC was proposed in the construction of the module. This solution eliminates non-profitable features of microsystem visible when using the configuration proposed by the manufacturer, e. g. the necessity of performing a calibration measurement, a too narrow range of the measured impedance modulus 1 kΩ ÷ 10 MΩ and the measurement frequency range 1 kHz ÷ 100 kHz.

The performed measurement of the reference two-terminal RC network using the realized prototype of the interface circuit proved the fulfilment of the assumed parameters. The relative error of two-terminal network impedance modulus measurement is in the range of ±1.6%, and the absolute error of the impedance argument is on the level ±0.6° (excluding the highest frequency point). The obtained accuracy is fully acceptable in case of impedance measurement of anticorrosion coating in the field. The comparison measurements performed with the aid of Solartron set of instruments showed that the impedance measurement accuracy of the proposed module is comparable to laboratory set of instruments.

The important advantage of the proposed solution based on AD5933 microsystems is lowering the power consumption down to approx. 0.7 W, which makes possible powering the measurement module from a PC using the +5 V voltage from the USB. It is a very profitable feature of the module designed to work directly in the field.

References

1. S. Skale, V. Doleček, M. Slemnik, Electrochemical impedance studies of corrosion protected surfaces covered by epoxy polyamide coating systems, Progress in Organic Coatings, Vol. 62, No 4 (2008) 387-392.
2. M. O'Donoghue, R. Garrett, V. Datta, P. Roberts, T. Aben, Electrochemical Impedance Spectroscopy: Testing Coatings for Rapid Immersion Service, Materials Performance, NACE International, (2003) 36-41.
3. G. Grundmeier, W. Schmidt, M. Stratmann, Corrosion protection by organic coatings: electrochemical mechanism and novel methods of investigation, Electrochimica Acta 45 (2000), 2515–2533.
4. T. Uchiyama, S. Ishigame, J. Niitsuma, Y. Aikawa, Y. Ohta, Multi-frequency bioelectrical impedance analysis of skin rubor with two-electrode technique, Journal of Tissue Viability, Vol. 17, No 4, (2008), 110-114.
5. Zhang Xu, Koon Gee Neoh, Anil Kishen, Monitoring acid-demineralization of human dentine by electrochemical impedance spectroscopy (EIS), Journal of Dentistry, Vol. 36, No 12, (2008) 1005-1012.
6. M. Min, T. Parve, An Electrical Bio-Impedance Analyzer for Implantable Medical Devices, IEEE IMTC (2005) 1823-1828.
7. J. Parilkowa, I. Krejci, J. Vesely, Two Non-invasive Methods of Dike Monitoring and Their Results, Proc. of 10-th IMEKO TC10 International Conference on Technical Diagnostics, Budapest Hungary (2005) 67-71
8. J. Parlikowa, J. Vesely, L. Procházka, EIS–Monitoring Method of the Earthen Dikes of Water Reservoirs, International Symposium on Water Management and Hydraulic Engineering, Ohrid/Macedonia, 1-5 September (2009) 729-740.
9. J. Parlikowa, J. Vesely, J. Pavlik, R. Stoklasek, Monitoring of the soil status using electrical impedance spectrometry method developed in project E!3838 of the Europe International Program EUREKA, XIX IMEKO World Congress Fundamental and Applied Metrology, Sept. 6-11 (2009) Lisbon, Portugal, 2234-2237.
10. L. Angrisani, A. Baccigalupi, and A. Pietrosanto, A Digital Signal-Processing Instrument for Impedance Measurement", IEEE Trans. on Instr. and Meas., Vol. 45, No 6 (1996) 930-934
11. J. Bordzilowski, K. Darowicki, S. Krakowiak, A. Krolikowska, Impedance measurements of coating properties on bridge structures, Progress in Organic Coatings, Vol. 46 (2003) 216-219.
12. J. R. Macdonald, LEVM Manual ver.7.11. CNLS Immittance Fitting Program. Solartron Group Limited 1999.

13. ZPlot for Windows, Electrochemical Impedance Software, Ver. 1.2, Operating Manual, Scribner Assoc. Inc., Charlottesville, Virginia 1995.
14. B. A. Boukamp, Equivalent circuit ver. 4.51, Netherlands, University of Twente, 1989.
15. Solartron, High Impedance Interface 1294 Operating Manual, Dec. 2001, Frequency Response Analyzer 1255.
16. Novocontrol, BETA Series Analyzer http://www.novocontrol.de/html/index_analyzer.htm.
17. Zahner, Electrochemical Workstation IM6, http://www.zahner.de/download/b_im6.pdf.
18. Analog Devices, AD5933 1 MSPS, 12-Bit Impedance Converter, Network Analyzer, 2005.
19. Analog Devices, Evaluation Board for the 1 MSPS 12-Bit, Impedance Converter Network Analyzer, Preliminary Technical Data EVAL-AD5933EB, 2005.
20. J. Hoja, G. Lentka, Portable analyzer for impedance spectroscopy. XIX IMEKO World Congress Fundamental and Applied Metrology, Sept. 6-11, 2009, Lisbon, Portugal, 497-502.
21. J. Hoja, G. Lentka, An analysis of a measurement probe for a high impedance spectroscopy analyzer. Measurement, vol.41, No. 1 (2008) 65-75.
22. Franco S., Operation amplifiers and analog integrated circuits. McGraw-Hill Book Company, 1988.
23. http://www.atlas-sollich.pl/eng/products/0441.htm